Journal of
Composites Science

MDPI

Article

Mechanical and Tribological Attributes of Al-CNT-Sn Composites Prepared by Press and Sintering

Vilas Dhore [1,2,*], Walmik Rathod [1] and Kashinath Patil [2]

[1] Department of Mechanical Engineering, Veermata Jijabai Technological Institute, Mumbai 400019, India; wsrathod@me.vjti.ac.in
[2] Department of Mechanical Engineering, K J Somaiya College of Engineering, Mumbai 400077, India; kashinath@somaiya.edu
* Correspondence: vilasdhore@me.vjti.ac.in or vilasdhore@somaiya.edu; Tel.: +91-22-6644-9522

Abstract: Carbon nanotubes (CNTs) have shown tremendous progress during the past two decades due to their extraordinary properties. With CNTs added as an alloying element, various engineering materials exhibit better mechanical properties. Multi-walled carbon nanotubes (MWCNT) were synthesized in-house by chemical vapor deposition process. Carbon nanotube-reinforced aluminum composites were prepared by cold pressing (or compaction) and sintering using different fractions (0.5, 1.0, 1.5, and 2.0 weight percent) of MWCNTs. The Al-CNT composites consists of tin (Sn) at 1.0 wt.% in each composition. Tin promotes the sintering of aluminum matrix composite. The effect of CNT on the density, hardness, and wear behavior of the composites were studied. Wear tests were performed to determine friction and wear under dry, wet, and hot conditions under varying loads from 5 N to 20 N. X-ray diffraction, Raman spectroscopy, scanning electron microscopy, and transmission electron microscopy techniques were used for the characterization. This investigation shows that increased CNT content significantly improves the hardness and wear resistance of the composites. The friction and wear were found to increase with operating temperature. A significant reduction in coefficient of friction and wear rate was observed with the application of oil during the wear test.

Keywords: aluminum; carbon nanotubes (CNT); composites; powder metallurgy; cold pressing; argon sintering; wear

Citation: Dhore, V.; Rathod, W.; Patil, K. Mechanical and Tribological Attributes of Al-CNT-Sn Composites Prepared by Press and Sintering. *J. Compos. Sci.* **2021**, *5*, 215. https://doi.org/10.3390/jcs5080215

Academic Editor: Francesco Tornabene

Received: 12 July 2021
Accepted: 9 August 2021
Published: 12 August 2021

1. Introduction

The carbon nanotubes (CNTs) are widely used as reinforcement materials in any matrix due to their extremely high strength and stiffness [1]. CNT's excellent mechanical and electrical properties have led to its use in metal, polymer, and ceramic matrix composites [2–4]. Aluminum is one of the crucial materials used in the automotive and aerospace industries [5,6]. The specific strength of the pure metal is lower than that of composites [7]. Many studies indicated that the inclusion of CNTs in aluminum matrix composites (AMCs) improved their mechanical properties [8–10]. Although CNTs exhibit excellent physical and mechanical properties, the main disadvantage of Al-CNT composites is the difficulty of dispersing reinforcement throughout the matrix [11]. Carbon nanotube-reinforced AMCs exhibit properties affected by chemical stability, distribution, and interfacial bonding between the CNTs in the matrix [5,12]. In order to achieve uniform dispersion of CNTs in composites, ball milling, magnetic stirring, and wet shake mixing methods have been adopted [13]. Upon ball milling at a certain speed and duration, the good dispersion of CNTs has been observed in the aluminum matrix [14,15]. According to Li et al., milling of Al powder with CNT-SiCp hybrid reinforcement for 60 min at a speed of 200 rpm resulted in an unformed dispersion of CNTs on the Al matrix [16]. The results of Peng and Chang show good dispersion of CNTs in an Al matrix with small agglomeration after 4 h of magnetic stirring followed by 30 min of wet shaking [17]. Kim

et al. investigated Al-CNT composites formed by hot pressing (HP) and spark plasma sintering (SPS), and they observed that SPS is a better method to minimize wear and friction [18]. As per Choi et al., increasing CNTs in Al composites up to 4.5 wt. % led to decreased wear rate and coefficient of friction and an increase in both parameters with the applied load [19]. Aluminum alloys produced by the powder metallurgy route enrich and strengthen with alloys such as tin, magnesium, iron, and lead. [20]. A low melting point for Sn in the composition causes liquid phase sintering of aluminum composites [21]. The powder metallurgy process operates at a temperature of 75 to 90% of the melting point of the matrix material [22]. In powder metallurgy, there are various fabrication techniques such as hot pressing [23], spark plasma sintering [24], cold pressing, and sintering [25].

This study focused on the preparation of Al-CNT-Sn composites using the cold compaction and argon sintering method by the powder metallurgy (PM) route. The Al-CNT-Sn composites with different CNT fractions were prepared to investigate the effects of CNT on density, hardness, and wear characteristics.

2. Materials and Methods

Aluminum and tin powders were purchased from Alpha Chemika, Mumbai, with a purity of >99.5% and a size of ~25 µm. MWCNTs were synthesized in-house using a chemical vapor deposition process. Figure 1 shows the morphology of as-received aluminum powder and their EDS scans.

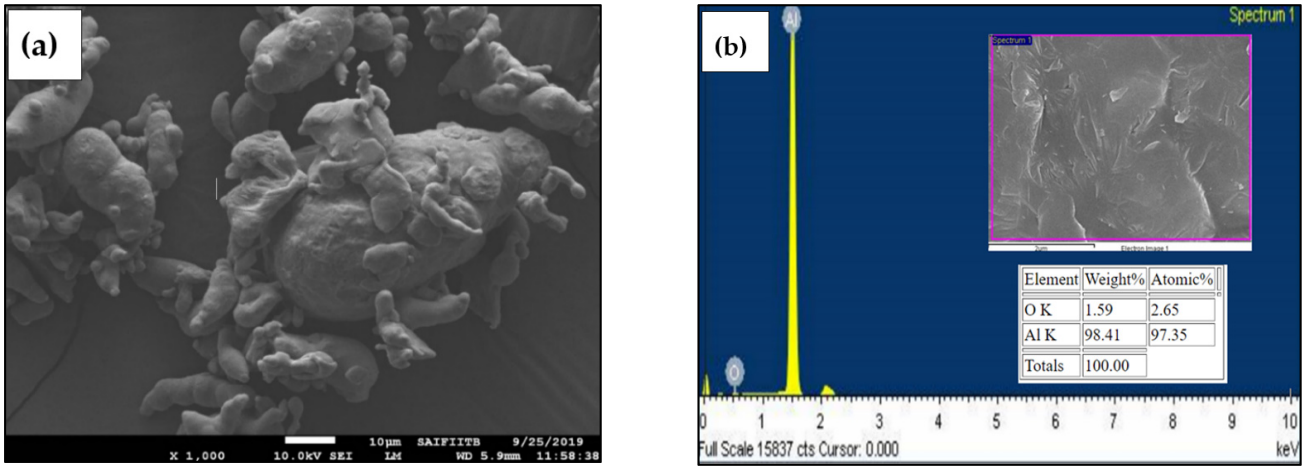

Figure 1. (**a**) SEM micrograph of aluminum powder (**b**) EDS scan of aluminum powder.

2.1. CNT Synthesis

The catalyst prepared with the wet impregnation method is Fe/Co/Ni/$CaCO_3$ with Fe, Co, and Ni as catalysts and $CaCO_3$ as the catalyst carrier. Fe $(NO_3)_3 \cdot 9H_2O$, Co $(NO_3)_2 \cdot 6H_2O$, Ni $(NO_3)_2 \cdot 6H_2O$ were used as catalyst precursors, and $CaCO_3$ substrate dissolved in water. Continuous stirring ensured the uniform mixing of nitrates and the substrate. The precipitates thus formed dried in an oven at 110 °C for 5 h. The catalysts were calcined in an argon environment at 700 °C for 20 min. The sample was then heated at 750 °C in a horizontal tube furnace under continuing argon flow for 40 min. Then acetylene gas was injected into the furnace for 30 min. Eventually, this led to the diffusion of carbon onto a metal catalyst, which ultimately led to the development of MWCNTs. During CNTs synthesis, the furnace maintains a controlled flow of 80 mL/min of acetylene and 60 mL/min of argon. In order to remove the amorphous carbon present in raw CNTs, they were first rinsed in Nitric acid and later with Hydrochloric acid. It was then washed with deionized water and dried for 2 h at 120 °C.

2.2. Milling

Aluminum powder, Sn (1.0 wt. %), and CNT with different weight fractions (0.5, 1.0, 1.5, and 2.0 wt. %) were pulverized in a RETSCH 100 planetary ball mill. A speed of 200 rpm for 60 min allowed to carry out the milling of powders. The machine was allowed to cool after 20 min of operation by pausing for 10 min to avoid overheating. Stainless steel balls of 10 mm diameter and the ball to powder ratio as 10:1 was chosen for milling [26]. The 2.0 wt. % stearic acid was used as a process control agent to keep away the excessive cold welding of powder during milling.

2.3. Fabrication of Al-CNT-Sn Composites

The milled Al-CNT-Sn powders with different CNT fractions were cold compacted at a pressure of 200, 300, 400, 500, and 600 MPa to investigate the compaction performance. The Al-CNT-Sn powder samples weighing 2.5 g were cold compacted in pellet dies of 10 mm diameter with a 50 kN hydraulic press. The silicon spray was applied to the die and punch to remove the specimen from the die after consolidation. Sintering was completed in a horizontal tube furnace at 530 °C with a 5 °C/min rate in an argon atmosphere and soaking for three hours. Figure 2a shows the process of fabrication. Figure 2b shows the sintered Al-CNT-Sn composite specimens.

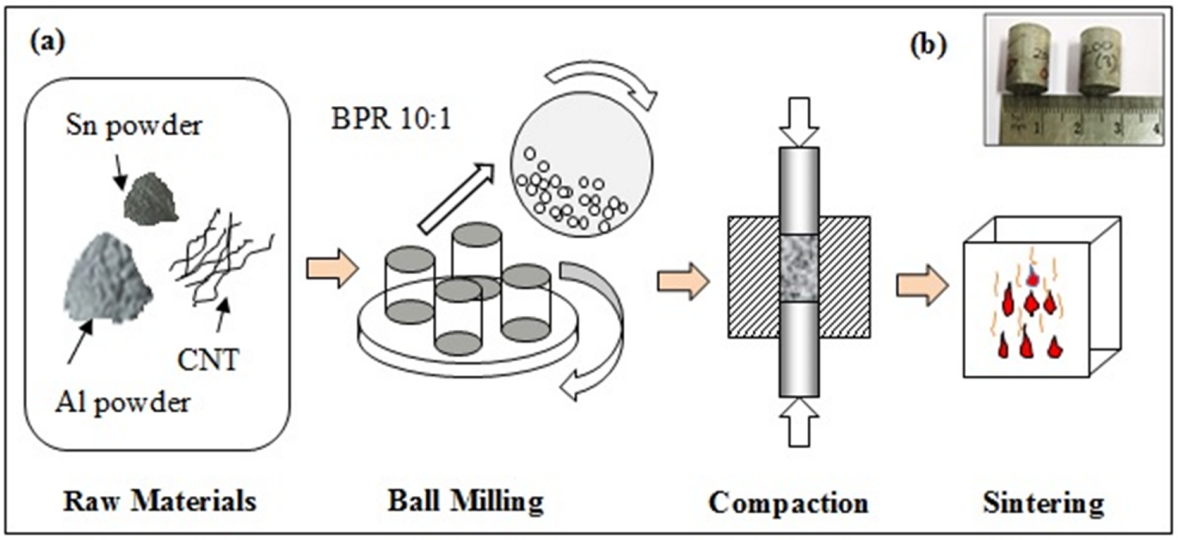

Figure 2. (**a**) A schematic representation of steps in consolidation of composites. (**b**) sintered Al-CNT-Sn Composites.

2.4. Characterization of CNT and Al-CNT-Sn Composites

The morphology of CNT was examined by a scanning electron microscope (JEOL JSM-7600F). High-resolution transmission electron microscopy (HRTEM) analysis was carried out on 300 kV FEI, Tecnai G2, F30 HRTEM. The X-ray diffraction (XRD) pattern of Al-CNT-Sn composites was examined by an Empyrean Malvern Panalytical diffractometer using Cu-Kα radiation at 40 kV potential with a scattering angle of $2\theta = 5^\circ$ to 90°. The wear tests were carried out on a pin on the disc tribometer manufactured by DUCOM, Bangalore (India). The counterpart disc was prepared with EN31 material for the wear test. Sai Kripa Engineering, Mumbai, manufactured the discs. The surface morphology of worn samples was detected using Zeiss Gemini SEM 300.

2.5. Wear Testing Process

The tribological tests were conducted on the pin-on-disc tribometer as per ASTM G99 standards. A pin prepared with an Al-CNT-Sn specimen of 10 mm diameter and 25 mm height was used on the pin-on-disc machine. The test was conducted on Al-CNT-Sn composite at various loads from 5 N to 20 N and a sliding speed of 0.5 m/s. The counter disc prepared from EN31 steel hardened to 50 HRC with a Ra value ranging from 0.8–1.0 μm.

Before every experiment, the disc was cleaned with acetone and dried. A wear study was carried out under three conditions: dry sliding, high temperature, and oil-lubricated. Dry sliding wear tests were conducted on an Al-CNT-Sn composite with varying CNT fractions from 0.5 to 2.0 wt. % CNTs at ambient temperature. The high-temperature wear tests were performed at 100, 200, 300, and 400 °C on Al-CNT-Sn samples with 1.0 wt. % CNT. The wet conditions wear tests were carried out with two oils, namely SAE 60 and diesel, at a constant flow of 0.25 L/min. During the wear test, the applied load on the pin varied from 5 to 20 N loads. Table 1 shows the specifications of the wear testing machine.

Table 1. Specifications: Pin on disc tribometer.

Pin on Disc Tribometer	
Disc size	165 mm diameter × 8 mm thick
Disc speed	1–2000 rpm (Accuracy: 1 + 1% of measured speed in rpm)
Load (N)	5–200 N
Temperature (°C)	Ambient 20 °C
Chamber temperature (°C)	Maximum 800 °C
Electricity required	230/1ϕ /50 Hz/6 A

3. Results

3.1. Characterization of Carbon Nanotubes

Figure 3a displays the scanning electron microscope (SEM) micrograph of as-synthesized CNT. SEM image reveals that the diameter of synthesized CNT is in the range of 20–25 nm with a length of few microns. Figure 3b shows the high-resolution TEM image of CNT. TEM shows approximately 20 walls in the as-synthesized CNT, confirming that nanotubes are multiwalled. Obtained nanotubes have bamboo-like internodes. The internodes present in the nanotubes enhance the strength of the CNTs. The number of walls of MWCNT depends upon the processing parameters, such as a catalyst, precursor, operating temperature, and residence time of precursor [27]. The XRD scan of MWCNT, shown in inset Figure 3a, illustrates the peaks (002) at 26° and (100) at 43° agree with typical graphitic structure. The CNT's quality is assessed using an HR800-UV confocal micro-Raman spectrometer from Horiba Jobin Yvon, Paris, France. The anti-Stokes scattering technique is used in Raman analysis. Figure 4 shows Raman spectra of synthesized MWCNT. The Raman spectra of synthesized CNT show D-Band at 1340 cm^{-1} and G -Band at 1580 cm^{-1}, with an I_D/I_G ratio of 1.04. The as-produced MWCNTs were crystalline.

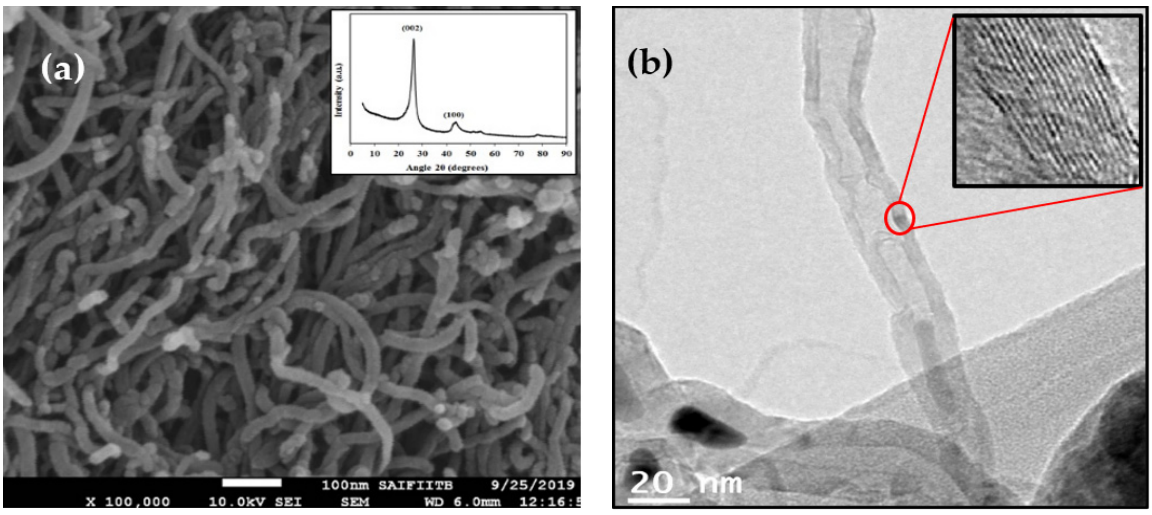

Figure 3. Characterization of MWCNTs: (**a**) scanning electron microscopy; (**b**) high-resolution transmission electron microscopy.

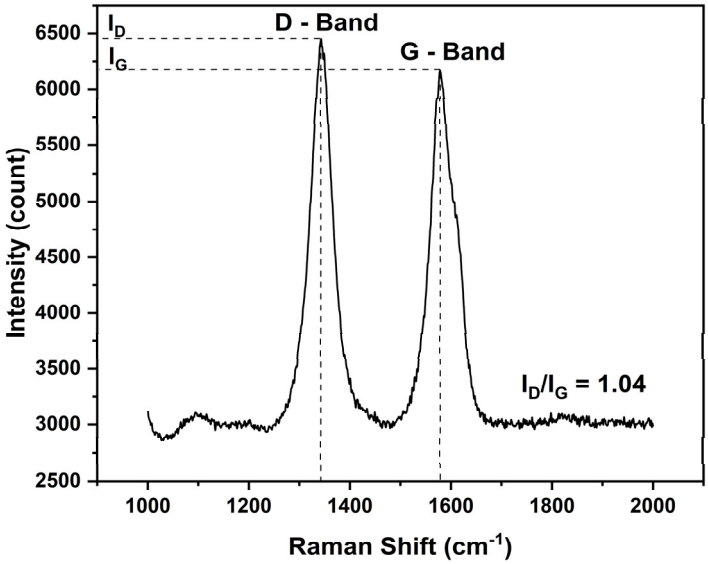

Figure 4. Raman spectroscopy of synthesized MWCNTs.

3.2. The Effect of CNT and Compaction Pressure on Density

The effect of the CNT fraction on the relative density of the sintered sample is depicted in Figure 5. The theoretical density (ρ_{th}) of the composite is calculated using the rule of the mixture. The density of CNT is assumed to be 1.6 gm/cc. The actual density (ρ_{act}) of composite specimens is calculated using mass per volume of the sample. The relative density is determined using the relation:

$$\rho_{rel} = \frac{\rho_{act}}{\rho_{th}} \times 100$$

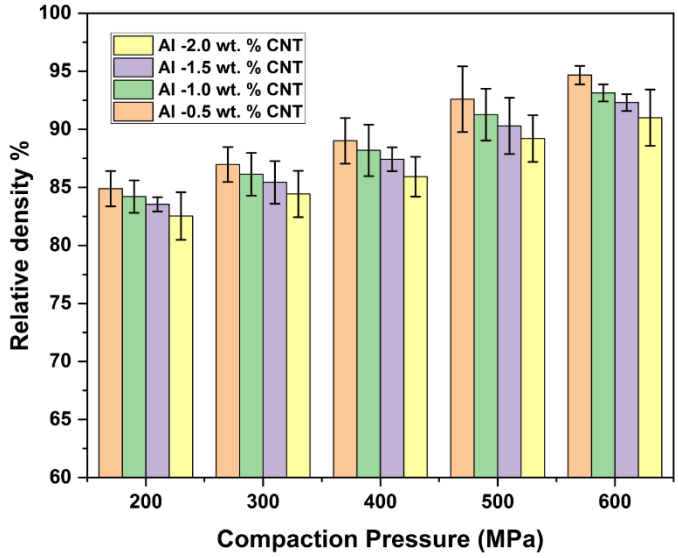

Figure 5. Effect of CNT content and compaction pressure on relative density of sintered compacts.

Figure 5 illustrates that as the CNT fraction increases in the specimen, the relative density declines. The reason behind this is an extremely low density of CNT as compared to aluminum and tin. It is seen that the density of composite improved with the increase in the compaction pressure applied during the specimen preparation during uniaxial pressing. The density of composites depends on various factors such as composition, size, and shape of mixture particle after milling and nature of dispersion of CNTs in the matrix. The Archimedes principle measured the bulk density of the specimen. The lowest

relative density, 82.5%, is observed in 2.0 wt. % CNT composites, prepared by compaction pressure of 200 MPa; however, the highest relative density, 94.3%, is noted at 0.5 wt. % CNT composites, prepared at a compaction pressure of 600 MPa.

3.3. Hardness

The microhardness of a material is a measure of its ability to withstand an applied load. The hardness of pure Al and Al-CNT-Sn composites is carried out on a Vickers microhardness tester (LECO LM700AT) as per ASTM E384 standards. The test was conducted at four different locations for each sample and averaged out. During an examination, the load is applied of 50 gm and a dwell time of 15 s. Figure 6 displays the microhardness at different compaction pressures for three-hour sintered samples. The investigation shows that the hardness of Al-CNT-Sn composites consistently improved with the increase in compaction pressure and CNT weight fraction. The hardness of pure Al increases by 25.81% when pressure is increased from 200 MPa to 600 MPa. With an increase in pressure from 200 to 600 MPa, the hardness of Al-CNT-Sn with 2.0 wt. % CNT is increased by 32%. As compaction pressure increases, the specimen becomes dense, and this improves the hardness in turn. The hardness of the sample, enhanced with the rise in CNT revealed from the results. By increasing CNT in Al from 0.5 to 2.0 wt. % at 600 MPa compaction pressure, the hardness of the Al-CNT-Sn composite increased by 22.85%. The solid interfacial bonds between the matrix and reinforcement and load sharing by CNT within the matrix contribute to improving the hardness of the composite. The sintering time also plays a significant role in improving the hardness [28]. The small volume of Al_4C_3 in Al-CNT-Sn composites observed in the XRD study also contributes to hardness enhancement. Table 2 reported the hardness and densities of Al-CNT composites fabricated through different processing routes by various researchers.

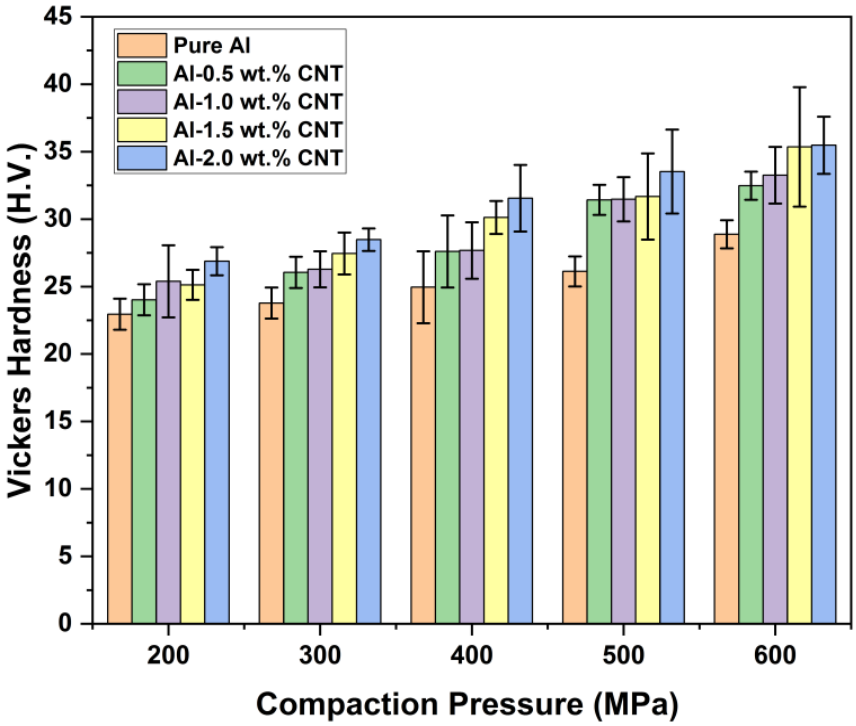

Figure 6. Effect of CNT content and compaction pressure on microhardness of sintered compacts.

Table 2. Reported hardness and densities of Al-CNT-Sn composites fabricated by different processes.

Authors	Material	Mixing	Fabrication Process	Hardness (HV)	Density
Nie et al. (2011)	Al powder 325 mesh, MWCNT 2 wt. %	Ball milling BPR 10:1, 100 rpm 8 h.	Spark plasma sintering 580 °C for 5 min at 40 MPa.	38	Relative density 95%
Bunakov et al. (2016)	Atomized Al size 5 µm, 1 wt. % MWCNT	Ultrasonic treatment and intensive stirring	Spark plasma sintering (SPS) at 600 °C at 60 MPa for 20 min.	46	-
Liu et al. (2016)	Al powder 250 mesh, 0.3 wt. % Graphene oxide	Mechanical stirring,	Cold compaction 560 MPa, sintered in inert gas at 600 °C	34	2.4 (g/cc)
Rahimian (2010)	Al powder 30 µm, Al_2O_3 powder 3 µm 10 wt. %	Ball milling BPR 10:1	Axial Pressing at 440 MPa, sintering at 550 °C for 45 min.	70	Relative density 97.5%
Kim et al. (2009)	Al powder, 3 wt. % CNT	Acid treatment and ultrasonication for 20 min.	SPS at 600 °C with the rate of 50 °C/min for 10 min at 50 MPa.	53.8	-
Bradbury et al. (2014)	Al powder, 2 wt. % MWCNT	Planetary milling BPR = 10:1, 350 rpm, 20 h	HP at 350 °C and 570 MPa for 10 s followed by extrusion at 550 °C with an extrusion ratio of 14:1	80	Relative density 95%
Present Work	Al powder, 1 wt. % Sn, 1.5 wt. % MWCNT	Planetary milling BPR = 10:1, 200 rpm, 1 h.	Cold pressing at 200 MPa to 600 MPa, sintering at 530 °C for 3 h	36	93.5%

3.4. Phase Analysis of Sintered Al-CNT-Sn Composites

Figure 7 shows XRD patterns of pure Al and Al-CNT-Sn composites. The primary aluminum peaks ate observed at 38.8°, 45°, 65.4°, and 78.5°. A small aluminum carbide (Al_4C_3) peak is noticed at 55.01°. However, the aluminum oxide (Al_2O_3) peak is not observed in the XRD scan. The Al-CNT-Sn composites reveal that increasing CNT content results in forming a small amount of an Al_4C_3 phase. The sources of formation of Al_4C_3 are CNT and stearic acid. Generally, during milling, due to structural damage on the CNT, this leads to amorphization. The interaction of damaged CNTs with the Al matrix leads to the formation of Al_4C_3 [29]. Moreover, stearic acid, which is added during milling as a process control agent, is a compound formed by carbon, hydrogen, and oxygen, which accounts for the formation of the Al_4C_3 phase [30].

3.5. Effect of Load on the Coefficient of Friction

Figure 8 shows the coefficient of friction as a function of the applied load and the CNT concentration in the composite. The wear test is carried out at a constant sliding speed of 0.5 m/s. The results show that the friction coefficient and wear loss increase with the increase in the applied load. The maximum coefficient of friction and wear loss is observed at an applied load of 20 N. Jagannathan et al. [31] investigated the coefficient of friction and wear rate of Al-CNT composites, prepared by cold compaction and hot extrusion for dry sliding wear. The authors reported that friction and wear rate decreased with an increase in CNT content when the load increased from 5 N to 20 N except for 2.0 wt. % CNT. The reported increase in the coefficient of friction and wear rate at 2.0 wt. % CNT

might be due to agglomeration occurred at higher CNT content. The quality of CNT, used for reinforcement and the uniform dispersion of CNT in the matrix, plays a crucial role in enhancing the properties of the composites. According to Bastwros et al., aluminum composite specimens with 5.0 wt. % CNT demonstrated a 48% reduction in coefficient of friction and 78% reduction in wear rate compared to the pure aluminum specimen. [32]. The present study reveals the decrease in the coefficient of friction and the wear loss with the increase in the CNT fraction in the Al composites. It is mainly due to the graphitic nature of CNT and the improved hardness of the Al-Sn-C composite with CNT added. Figure 9 shows the wear loss of Al-Sn-C composite samples with a load varying from 5 N to 20 N.

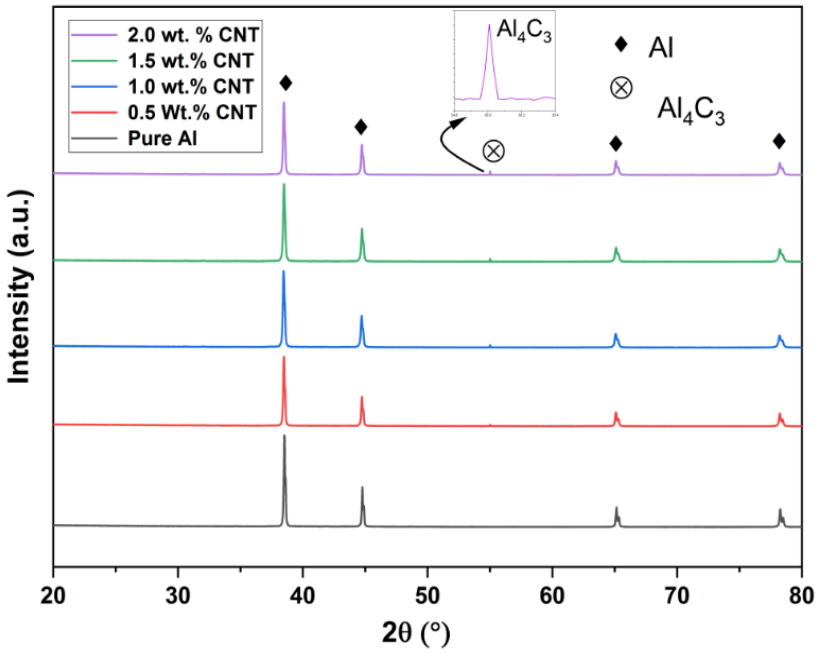

Figure 7. XRD scan of Al-CNT-Sn composites with different CNT fraction.

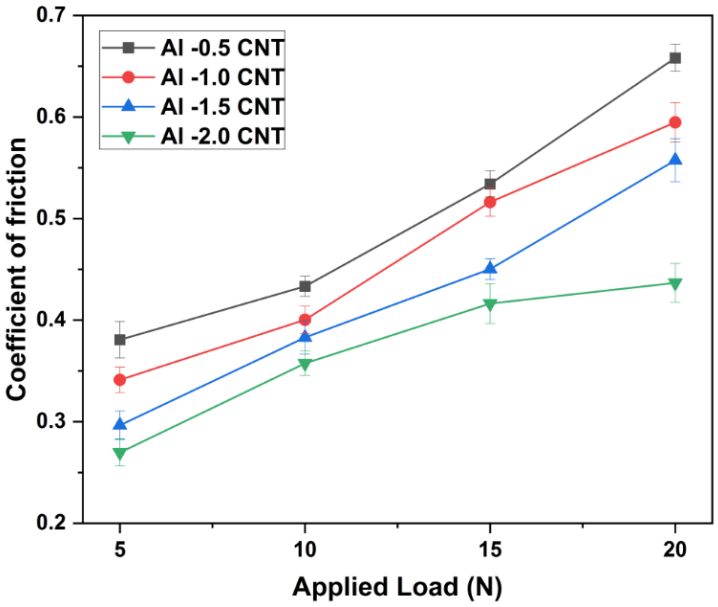

Figure 8. Effect of applied load on coefficient of friction for composite samples prepared with different CNT content in dry sliding condition.

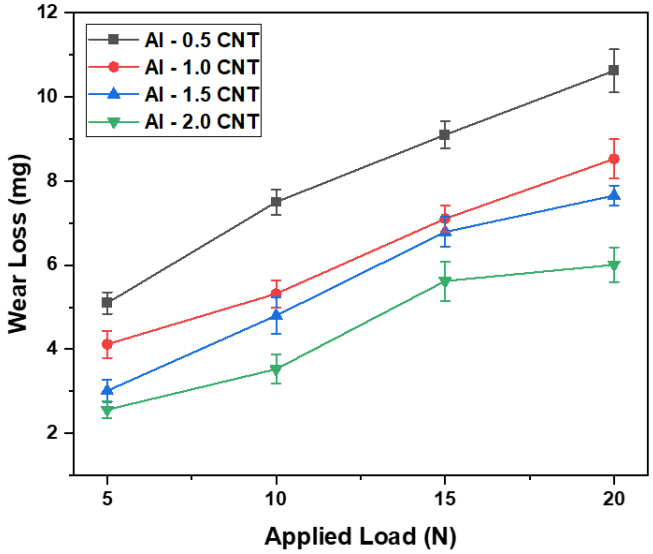

Figure 9. Effect of applied load on wear loss for composite samples prepared with different CNT content in dry sliding condition.

Figure 10 depicts how the coefficient of friction increases with an increase in the operating temperature of the sample. We studied Al-CNT-Sn samples with 1.0 wt. % CNT under a range of load conditions and operating temperatures. Theoretically, the coefficient of friction should decrease with an increase in operating temperature as the material softens at a higher temperature. In this case, the increment in friction coefficient might be due to the hardening effect of the specimen caused by the surge in temperature. An equal increment in coefficient of friction is noticed with an increase in test temperature by Jagannathan et al. and Kumar et al. [32,33]. Figure 11 displays the increase in wear loss with the increase in operating temperature and the applied load.

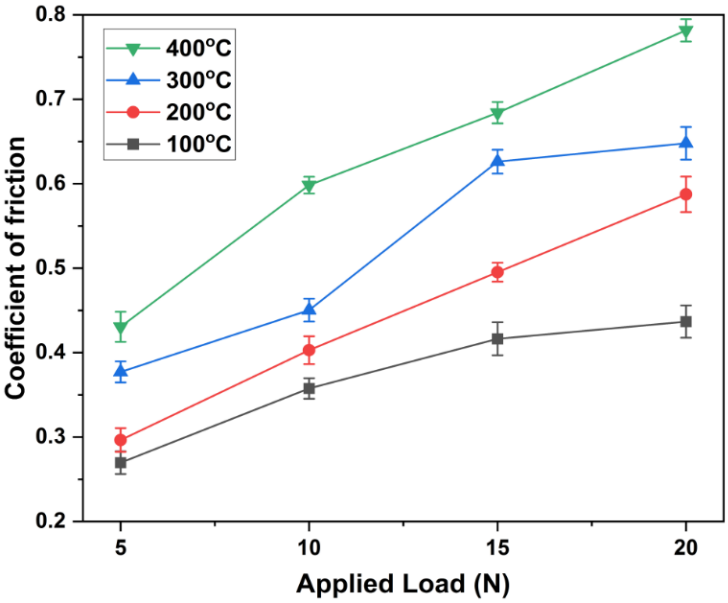

Figure 10. Effect of applied load on coefficient of friction at different temperature for Al–CNT-Sn specimens with 1.0 wt. % CNT.

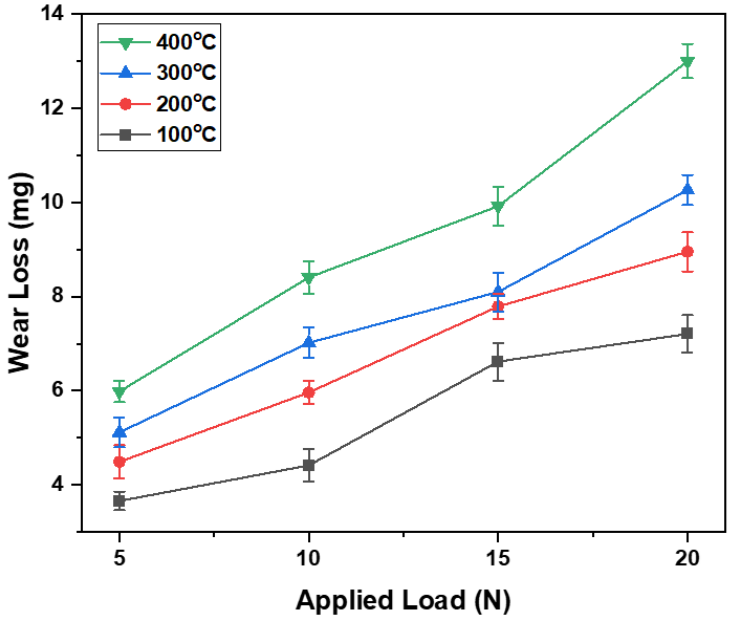

Figure 11. Effect of applied load on wear loss at different temperature for Al–1.0 CNT-1.0Sn specimens with 1.0 wt. % CNT.

The wet wear test was conducted with SAE 60 and diesel at room temperature on Al–CNT-Sn samples with 1.0 wt. % CNT. It is found that wet conditions create a lower coefficient of friction and wear than dry conditions. A lower coefficient of friction and wear occurs due to lubrication between the pin and disc, caused by oil. The lowest coefficient friction, 0.011, and wear loss of 0.027 mg are noticed for SAE 60 oil for 5 N load. With diesel, the coefficient of friction and wear loss is witnessed higher compared to SAE 60 oil. As with dry sliding conditions, with increasing load, friction and wear loss increase for wet conditions. The SAE 60 oil has better lubricating properties as compared with diesel which is primarily fuel. The coefficient of friction and wear loss comparison of SAE 60 oil and diesel oil is shown in Figures 12 and 13, respectively.

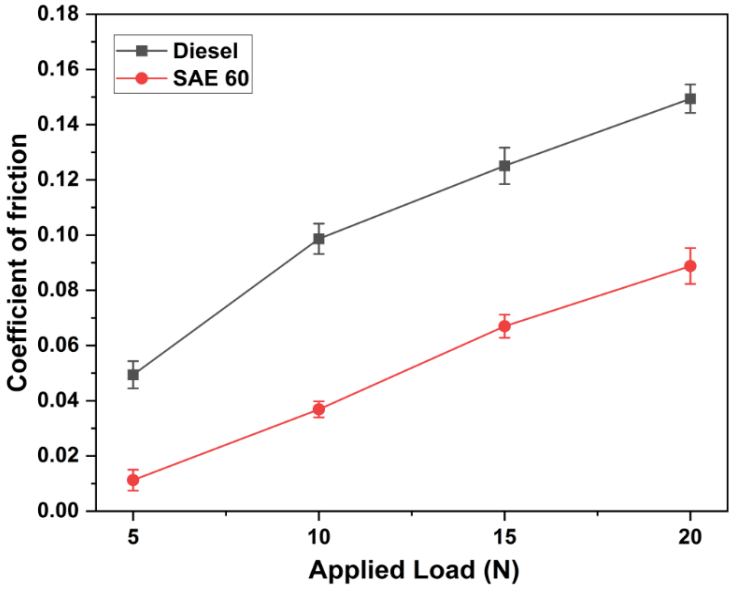

Figure 12. Effect of applied load on coefficient of friction in wet condition for Al-CNT-Sn specimens with 1.0 wt. % CNT.

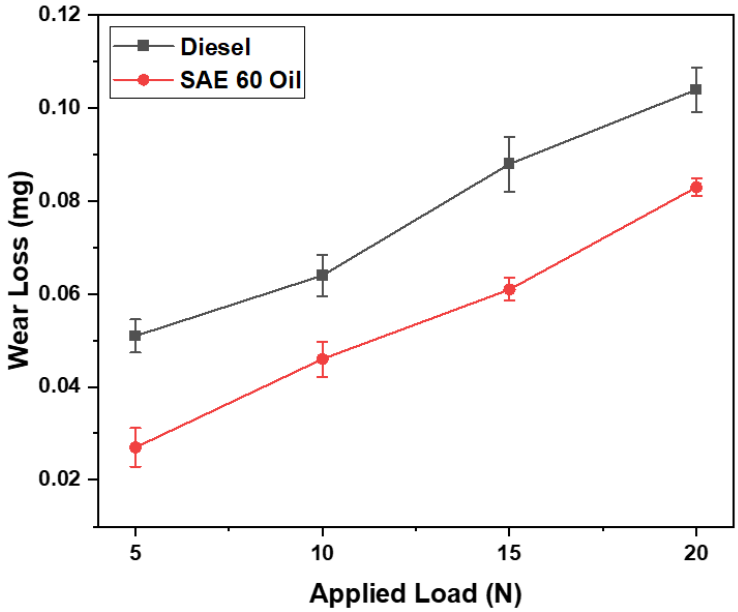

Figure 13. Effect of applied load on coefficient of friction in wet condition for Al-CNT-Sn specimens with 1.0 wt. % CNT.

Figure 14a–d shows the SEM images of wear specimens of Al-CNT-Sn composite with 1.0 wt. % CNT at 5, 10, 15, and 20 N loads, respectively. SEM micrographs in Figure 14a,b reveal slight delamination and tiny grooves tested at a lower load of 5 N and 10 N, respectively, at room temperature. Figure 14c,d noticed that delamination and micro ploughing on the worn surfaces increased with the increase in applied load. Surface damage is more consistent with the increase in applied load. Figure 14e–h shows SEM morphologies of specimens with the tribological test carried out under high operating temperatures varying from 100 to 400 °C and at an applied load of 20 N. The worn surfaces show the ploughing marks and grooves in the direction of sliding. The specimen of 300 °C shown in Figure 14g reveals adhesive wear with severe surface damage at several locations. The SEM of the composite at 400 °C revealed the oxidation wear due to higher temperature. Due to oxidation, severe surface damage is noted on the sample surface, which shows more wear rate. As discussed in the previous paper, Al-CNT-Sn composite surfaces with lower CNT fractions show more wear rate. A more significant amount of wear loss is observed due to delamination and deep ploughing [28]. On the contrary, reduced wear and wear friction coefficient is noticed with the CNT fraction in the composite sample.

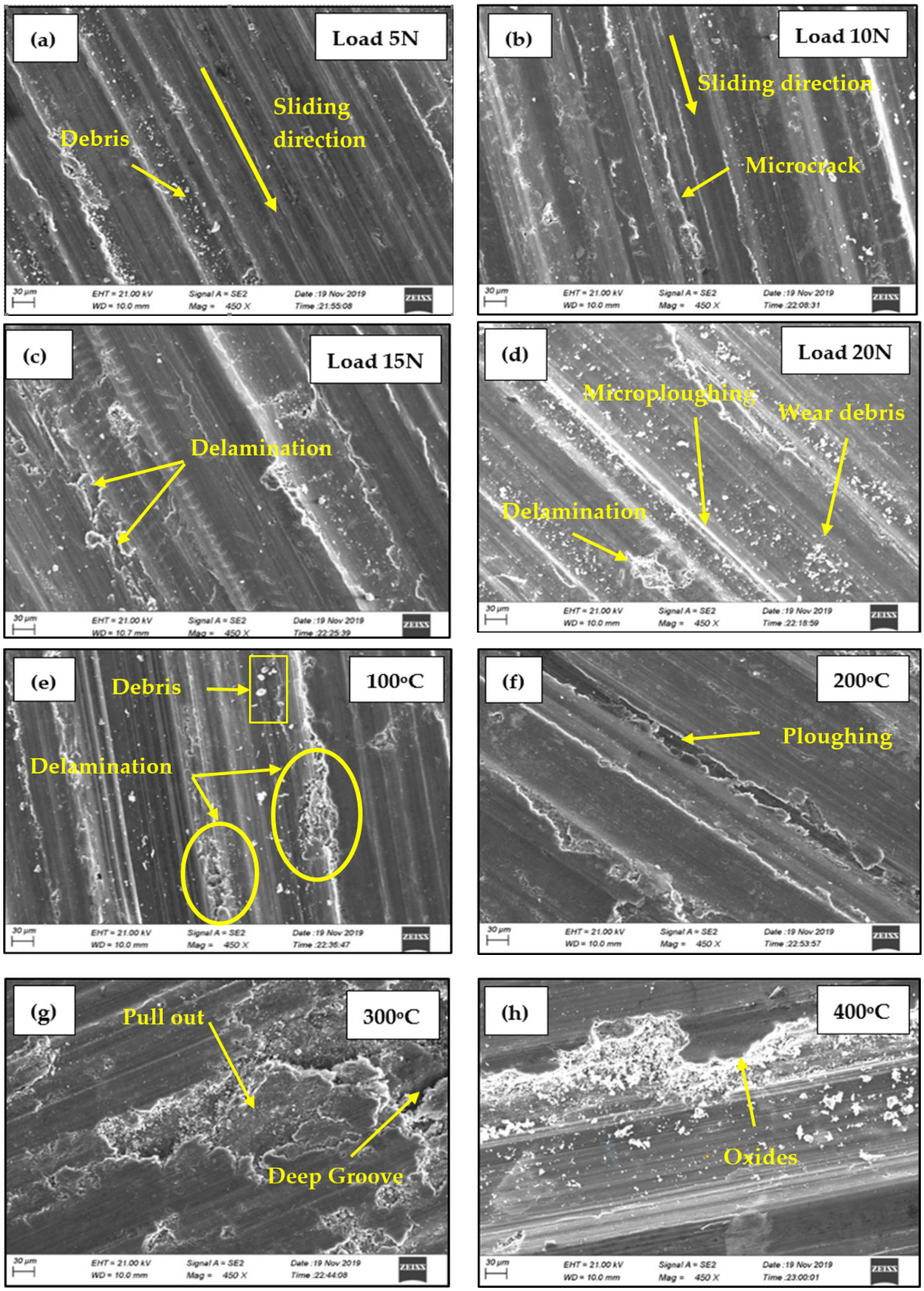

Figure 14. SEM images of worn samples of Al-CNT-Sn composite with 1.0 wt. % CNT: (**a**) dry sliding wear with 5 N load at room temperature (RT); (**b**) dry sliding wear with 10 N load at RT; (**c**) dry sliding wear with 15 N load at RT; (**d**) dry sliding wear with 20 N load at RT; (**e**) wear at 100 °C with 20 N load; (**f**) wear at 200 °C with 20 N load; (**g**) wear at 300 °C with 20 N load; (**h**) wear at 400 °C with 20 N load.

4. Conclusions

In this study, the density, hardness, and tribological properties of Al-CNT-Sn composites were studied under dry, high temperature, and oil-lubricated conditions. Based on the investigations, the following conclusions were drawn:

Carbon nanotube-reinforced aluminum composites were prepared using a cold pressing and sintering technique. The hardness and density of the prepared Al-CNT-Sn composites are lower than the composites prepared with other processing routes such as hot pressing, hot extrusion, and spark plasma sintering. The hardness of the pure Al sample increases by 25.81% when the compaction pressure is raised from 200 MPa to 600 MPa. Following this, an increase in the CNT content from 0.5 to 2.0 wt. % at 600 MPa compaction pressure resulted in the hardness of the Al-CNT-Sn composite improving by 22.85%. The reported Al_4C_3 phase in the composite contributes to this aforementioned improvement. In composites, the density is directly proportional to the compaction pressure, while being inversely proportional to the CNT content in the composite. The experimental results showed that the addition of CNT has a significant impact on the friction and wear properties of the composite. The self-lubricating property of CNT accounted for a reduction of said friction and wear properties of Al composites. The results, exhibited by the tribological test suggest that temperature has a direct effect on the coefficient of friction and on the wear rate. While increasing the load during the wear test, both the friction coefficient as well as the wear rate also increased. Temperature-dependent surface damage can be seen in the SEM images. In the case of oil lubrication conditions, the observed friction and wear rate are significantly lower than dry sliding condition.

Author Contributions: Conceptualization, methodology, investigation, formal analysis, writing—original draft preparation, Review and editing V.D.; Conceptualization, methodology, Supervision, W.R.; Conceptualization, Writing—review and editing, K.P. All authors have read and agreed to the published version of the manuscript.

Funding: This research received no external funding.

Acknowledgments: Authors are thankful to K J Somaiya College of Engineering and Veermata Jijabai Technological Institute for providing the laboratory facility. We are also grateful to IIT Bombay for providing the characterization facility.

Conflicts of Interest: The authors declare no conflict of interest.

References

1. Harris, P. Carbon nanotube composites. *Inter. Mater. Rev.* **2004**, *49*, 39–43. [CrossRef]
2. Pradhan, S.; Datta, A.; Chatterjee, A.; De, M.; Chakravorty, D. Synthesis of aluminium matrix composites containing nanocrystalline oxide phases. *Bull. Mater. Sci.* **1994**, *17*, 849–853. [CrossRef]
3. Ram, H.; Koppad, P.; Kashyap, K. Influence of multiwalled carbon nanotubes on the aging behavior of AA 6061 alloy matrix nanocomposites. *Trans. Indian Inst. Met.* **2014**, *67*, 325–329.
4. Ahmad, I.; Kennedy, A.; Zhu, Y. Wear resistant properties of multi-walled carbon nanotubes reinforced Al_2O_3 nanocomposites. *Wear* **2010**, *269*, 71–78. [CrossRef]
5. Bakshi, S.; Agarwal, A. An analysis of the factors affecting strengthening in carbon nanotube reinforced aluminum composites. *Carbon* **2010**, *49*, 533–544. [CrossRef]
6. Liu, Z.; Zhao, K.; Xiao, B.; Wang, W.; Ma, Z. Fabrication of CNT/Al composites with low damage to CNTs by a novel solution-assisted wet mixing combined with powder metallurgy processing. *Mater. Des.* **2016**, *97*, 424–430. [CrossRef]
7. Liu, J.; Khan, U.; Coleman, J.; Fernandez, B.; Rodriguez, P.; Naher, S.; Brabazon, D. Graphene oxide and graphene nanosheet reinforced aluminium matrix composites: Powder synthesis and prepared composite characteristics. *Mater. Des.* **2016**, *94*, 87–94. [CrossRef]
8. George, R.; Kashyap, K.; Rahul, R.; Yamdagni, S. Strengthening in carbon nanotube/aluminium (CNT/Al) composites. *Scr. Mater.* **2005**, *53*, 1159–1163. [CrossRef]
9. Choi, H.; Kwon, G.; Lee, G.; Bae, D. Reinforcement with carbon nanotubes in aluminum matrix composites. *Scr. Mater.* **2008**, *59*, 360–363. [CrossRef]
10. Esawi, A.; Morsi, K.; Sayed, A.; Taher, M.; Lanka, S. Effect of carbon nanotube (CNT) content on the mechanical properties of CNT-reinforced aluminium composites. *Compos. Sci. Technol.* **2010**, *70*, 2237–2241. [CrossRef]

11. Batista, L.; Felisberto, M.; Silva, L.; Cunha, T.; Mazzer, E. Influence of multi-walled carbon nanotubes reinforcements on hardness and abrasion behaviour of porous Al-matrix composite processed by cold pressing and sintering. *J. Alloys Compd.* **2019**, *791*, 96–99. [CrossRef]
12. Chaudhary, S.; Singh, K.; Venugopal, R. Effect of Using Carbon Nanotubes on ILSS of Glass Fiber-Reinforced Polymer Laminates. *Trans. Indian Inst. Met.* **2018**, *71*, 3029–3036. [CrossRef]
13. Li, H.; Fan, J.; Kang, J.; Zhao, N.; Wang, X.; Li, B. In-situ homogeneous synthesis of carbon nanotubes on aluminum matrix and properties of their composites. *Trans. Nonferrous Met. Soc. China* **2014**, *24*, 2331–2336. [CrossRef]
14. Deng, C.; Wang, D.; Zhang, X.; Li, A. Processing and properties of carbon nanotubes reinforced aluminum composites. *Mater. Sci. Eng. A* **2007**, *444*, 138–145. [CrossRef]
15. Liu, Z.; Xu, S.; Xiao, B.; Xue, P.; Wang, W.; Ma, Z. Effect of ball-milling time on mechanical properties of carbon nanotubes reinforced aluminum matrix composites. *Compos. Part A Appl. Sci. Manuf.* **2012**, *43*, 2161–2168. [CrossRef]
16. Li, S.; Su, Y.; Ouyang, Q.; Zhang, D. In-situ carbon nanotube-covered silicon carbide particle reinforced aluminum matrix composites fabricated by powder metallurgy. *Mater. Lett.* **2016**, *167*, 118–121. [CrossRef]
17. Peng, T.; Chang, I. Uniformly dispersion of carbon nanotube in aluminum powders by wet shake-mixing approach. *Powder Technol.* **2015**, *284*, 32–39. [CrossRef]
18. Kim, I.; Lee, J.; Lee, G.; Baik, S.; Kim, Y.; Lee, Y. Friction and wear characteristics of the carbon nanotube-aluminum composites with different manufacturing conditions. *Wear* **2009**, *267*, 593–598. [CrossRef]
19. Choi, H.J.; Lee, S.M.; Bae, D.H. Wear characteristic of aluminum-based composites containing multi-walled carbon nanotubes. *Wear* **2010**, *270*, 12–18. [CrossRef]
20. Özay, Ç.; Gencer, E.; Gökçe, A. Microstructural properties of sintered Al-Cu-Mg-Sn alloys. *J. Therm. Anal. Calorim.* **2018**, *134*, 23–33. [CrossRef]
21. Schaffer, G.; Sercombe, T.; Lumley, R. Liquid phase sintering of aluminium alloys. *Mater. Chem. Phys.* **2001**, *67*, 85–91. [CrossRef]
22. Bunakov, N.; Kozlov, D.; Golovanov, V.; Klimov, E.; Grebchuk, E.; Efimov, M.; Kostishko, B. Fabrication of multi-walled carbon nanotubes-aluminum matrix composite by powder metallurgy technique. *Results Phys.* **2016**, *6*, 231–232. [CrossRef]
23. Kallip, K.; Babu, N.; AlOgab, K.; Kollo, L.; Maeder, X.; Arroyo, Y.; Leparoux, M. Microstructure and mechanical properties of near net shaped aluminium/alumina nanocomposites fabricated by powder metallurgy. *J. Alloys Compd.* **2017**, *714*, 133–143. [CrossRef]
24. Ujah, C.; Popoola, A.; Popoola, O.; Aigbodion, V. Optimisation of spark plasma sintering parameters of Al-CNTs-Nb nanocomposite using Taguchi Design of Experiment. *J. Mater. Sci.* **2019**, *100*, 14064–14073. [CrossRef]
25. Rahimian, M.; Ehsani, N.; Parvin, N. The effect of particle size, sintering temperature and sintering time on the properties of Al-Al_2O_3 composites, made by powder metallurgy. *J. Mater. Process. Technol.* **2009**, *209*, 5387–5393. [CrossRef]
26. Nie, J.; Jia, C.; Shi, N.; Zhang, Y.F.; Li, Y.; Jia, X. Aluminum matrix composites reinforced by molybdenum-coated carbon nanotubes. *Int. J. Miner. Metall. Mater.* **2011**, *18*, 695–702. [CrossRef]
27. Ramaraj, H.; Madiga, J.; Elangovan, H.; Haridoss, P.; Sharma, C. Homogenization for Dispersion and Reduction in Length of Carbon Nanotubes. *Trans. Indian Inst. Met.* **2017**, *70*, 2629–2639. [CrossRef]
28. Dhore, V.; Rathod, W.; Patil, K. Fabrication and Characterization of Cold-Pressed and Sintered Aluminium-MWCNT Composites. *Mater. Sci. Forum* **2021**, *1025*, 60–68. [CrossRef]
29. Bustamante, R.; Yoshida, M.; Sánchez, R.; Martinez, J.; Cantu, J. Al_4C_3 formation in carbon nanotube/Aluminum composites. *Microsc. Microanal.* **2012**, *18*, 1914–1915. [CrossRef]
30. Ostovan, F.; Amin, K.; Toozandehjani, M. Effects of CNTs content and milling time on mechanical behavior of MWCNT-reinforced aluminum nanocomposites. *Mater. Chem. Phys.* **2015**, *160*, 160–166. [CrossRef]
31. Jagannatham, M.; Saravanan, M.; Sivaprasad, K.; Babu, S. Mechanical and Tribological Behavior of Multiwalled Carbon Nanotubes-Reinforced AA7075 Composites Prepared by Powder Metallurgy and Hot Extrusion. *J. Mater. Eng. Perform.* **2018**, *27*, 5675–5688. [CrossRef]
32. Bastwros, M.; Esawi, A.M.; Wifi, A. Friction and wear behavior of Al-CNT composites. *Wear* **2013**, *307*, 164–173. [CrossRef]
33. Kumar, P.; Kumaran, S.; Rao, T.; Natarajan, S. High temperature sliding wear behavior of press-extruded AA6061/fly ash composite. *Mater. Sci. Eng. A* **2010**, *527*, 1501–1509. [CrossRef]